Supplementary Information (SI) for Journal of Materials Chemistry B.

SERS Active Silk Silver Films as a Platform for Osteogenic Biomarker Detection

Namrata Tiwari,[1] Manleen Kaur,[1] Ritu Das,[2] Nitish Kumar,[1] Neetu Singh[1,3]*

[1]Centre for Biomedical Engineering, Indian Institute of Technology Delhi, Hauz Khas, New Delhi 110016, India

[2] Department of Mechanical Engineering, Koç University, Rumelifeneri Yolu, Sariyer, Istanbul 34450 Turkey

[3]Biomedical Engineering Unit, All India Institute of Medical Sciences, Ansari Nagar, New Delhi 110029, India

*Corresponding authors: N. Singh: sneetu@cbme.iitd.ac.in

Study	Silk Source / Matrix	Ag Incorporation Strategy	Ag Size / Morphology	Primary Functionality	Limitations in Prior Work	What Is New in Your Platform
He et al., 2017 (Sericin–AgNPs)	Sericin solution	Light-assisted reduction of $AgNO_3$ by sericin tyrosine residues	20–40 nm AgNPs	Antibacterial, stable colloidal AgNPs	No structural matrix; no spatial control; no sensing capability; no atomic-scale confinement	Silk fibroin solid matrix enabling nanocluster confinement + SERS hotspot generation
Al Masud et al., 2021 (Sericin–AgNPs)	Sericin extract	Sericin acts as reducer and stabilizer	20–70 nm AgNPs	Antibacterial against MDR pathogens	Large particles; aggregation; antibacterial only; no controlled nanoscale clustering	Sub-50-nm clusters embedded within β-sheet domains → controllable, homogeneous distribution
Hydroxyapatite/Ag @ Silk Fibroin Coating (ACS Omega 2021)	Silk fibroin coating with nHA	UV-triggered AgNP growth on nHA nucleation sites	~40 nm AgNP or nHA/Ag complexes	Bone implants, antibacterial + osteogenic	Large AgNPs; rough coatings; no optical functionality; no nanoscale SERS hotspots	Smooth SF film with dispersed clustered Ag species enabling high-sensitivity SERS
Silk Fibroin–AgNP films (various wound healing systems)	Silk fibroin or composite	Chemical reduction or green synthesis	10–100 nm particles, broad	Antimicrobial, wound-healing matrices	Focus only on antibacterial; no spectroscopic function; polydisperse Ag	Highly monodisperse Ag clusters (0.25–0.5%) proven by DLS homogeneity
Review of Silk–Ag composites (Biomimetics 2025)	Various (SF, sericin)	Summary of green AgNP synthesis	5–100 nm	Antibacterial biomaterials	No SERS systems exist; no embedded nanocluster platforms; no biomarker detection	First demonstration of immobilized Ag nanoclusters within silk for biomarker-specific SERS

Table ST1: Comparative analysis of previously reported silk–silver nanoparticle (AgNP) systems and the novelty of the present silk silver film platform[1–5].

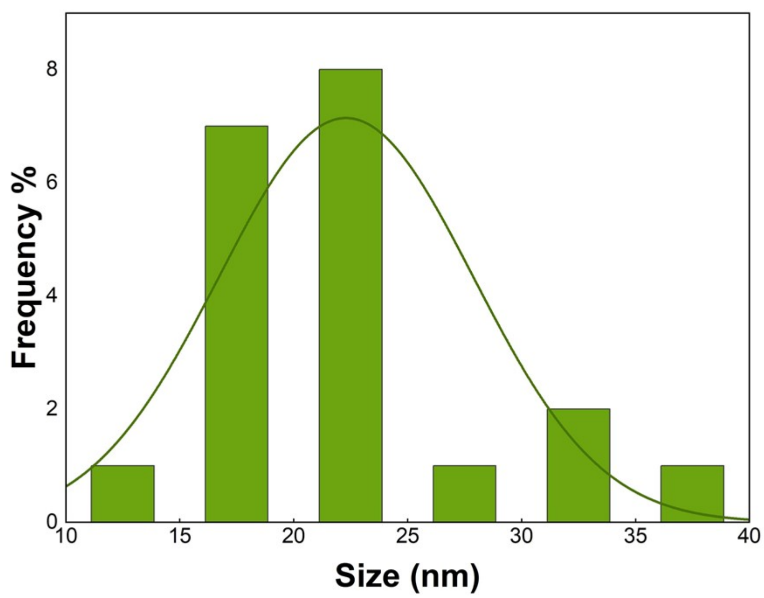

Figure S1: Particle size distribution of silver nanoclusters formed in the 0.5% silk silver fibroin solution. Histogram analysis shows that most nanoclusters fall within the 18–25 nm range, with a Gaussian fit indicating a narrow and unimodal size distribution. The frequency distribution confirms uniform nucleation and controlled growth of silver nanoclusters within the silk fibroin matrix.

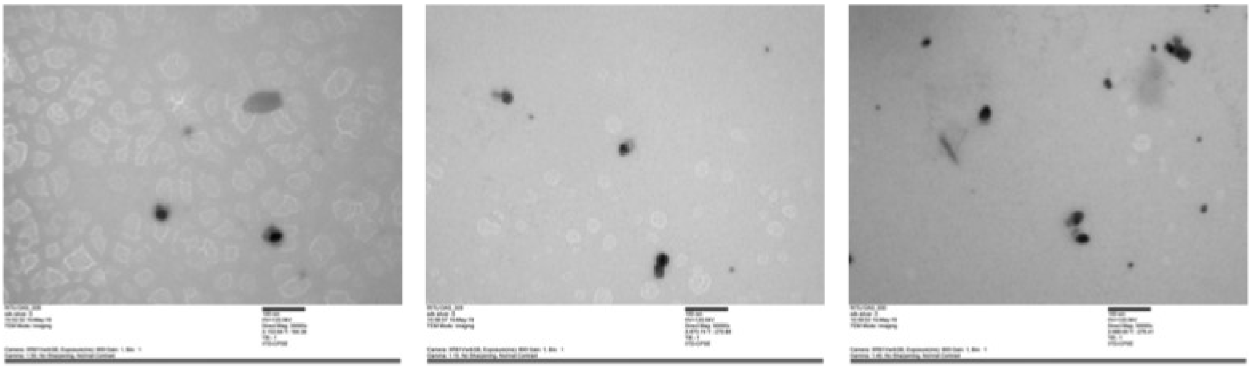

Figure S2: TEM micrographs of silver nanoclusters synthesized within the silk fibroin matrix at 0.5% silver concentration. (Scale: 100 nm).

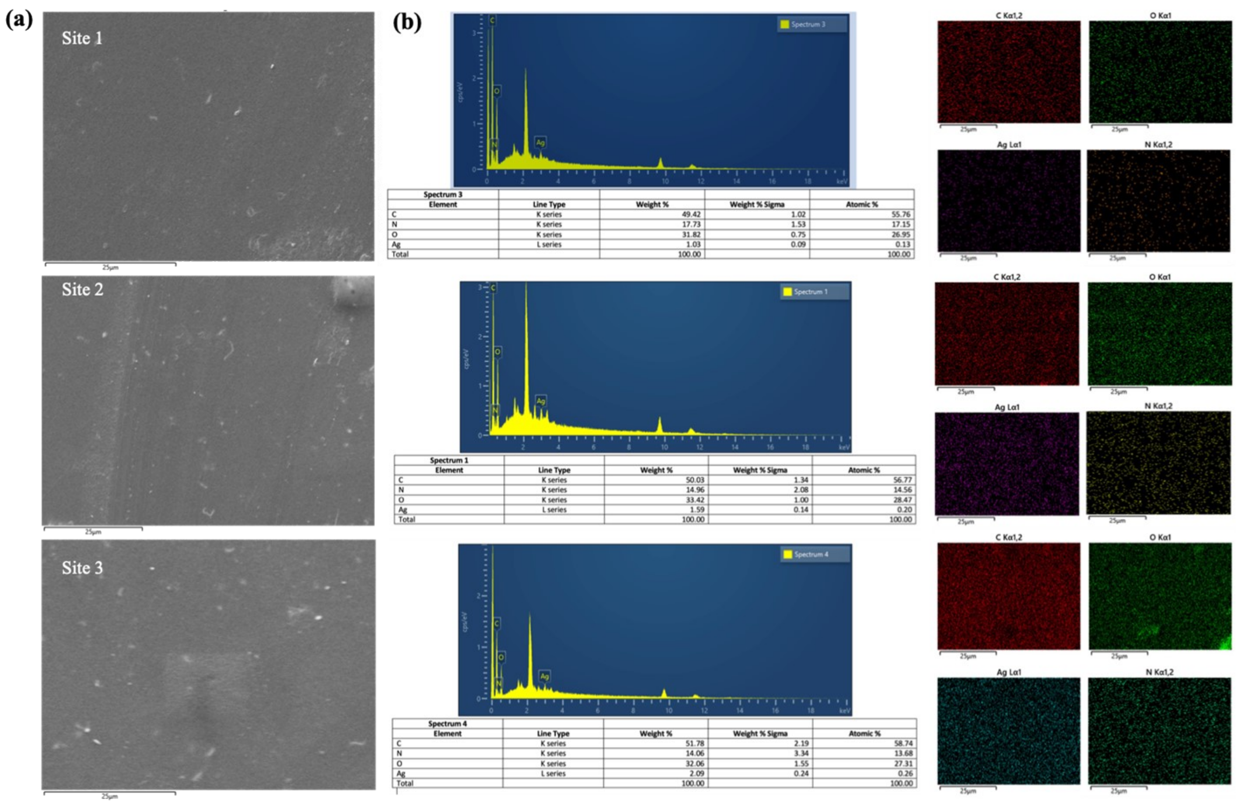

Figure S3: (a) FESEM micrographs and corresponding EDX spectra collected from three different regions (Site 1, Site 2, and Site 3) of the 0.5% silk silver film, and (b) EDX analysis confirms the presence of Ag along with the expected silk-derived elements (C, N, O) at all sites. Showing Ag content at surface (1.03–2.89 wt%), its consistent detection across multiple regions with elemental mapping indicates homogeneous nanocluster incorporation throughout the silk matrix.

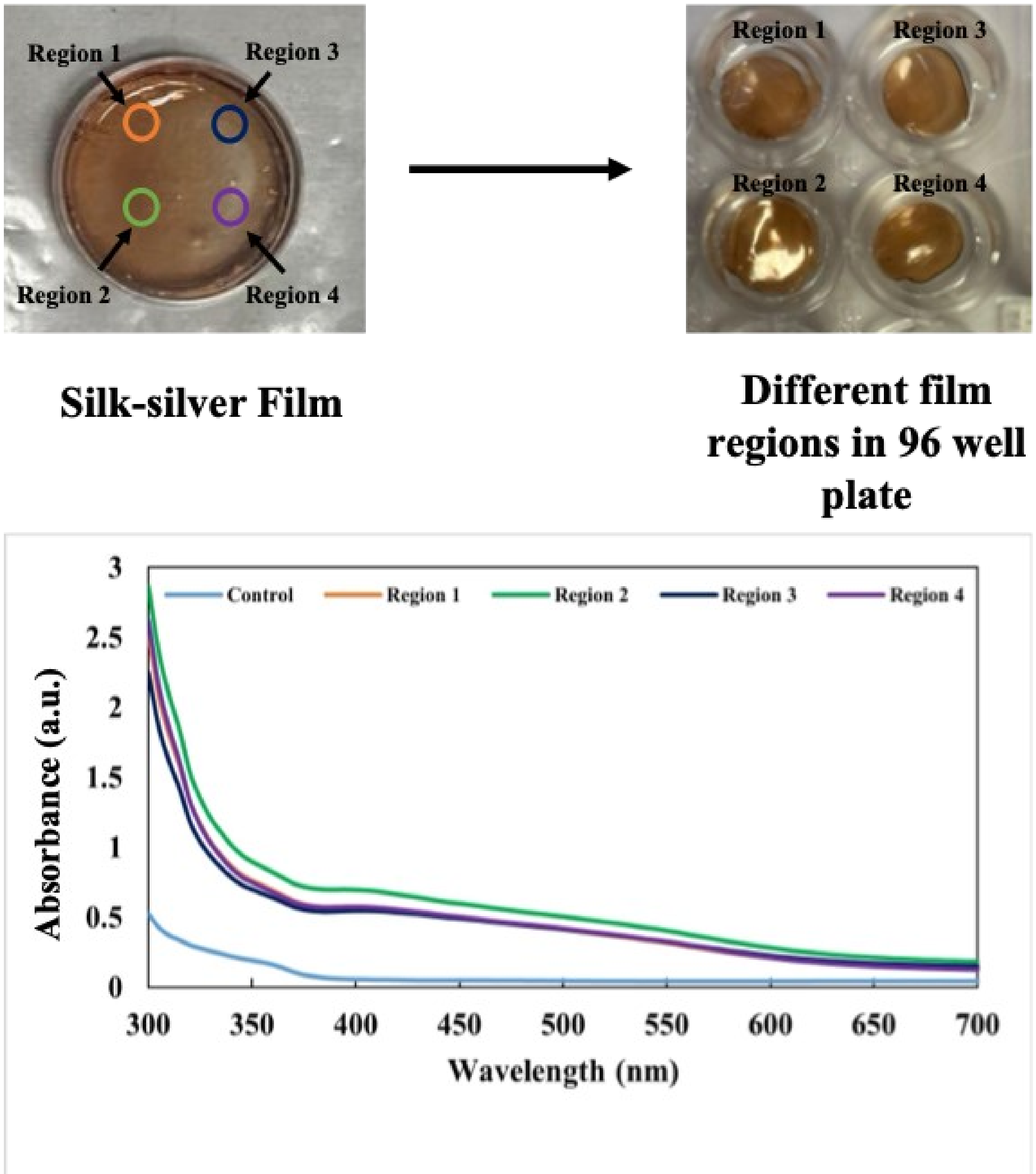

Figure S4: UV–*Vis* absorbance spectra of samples collected from different regions of the silk silver film with control as pure silk film.

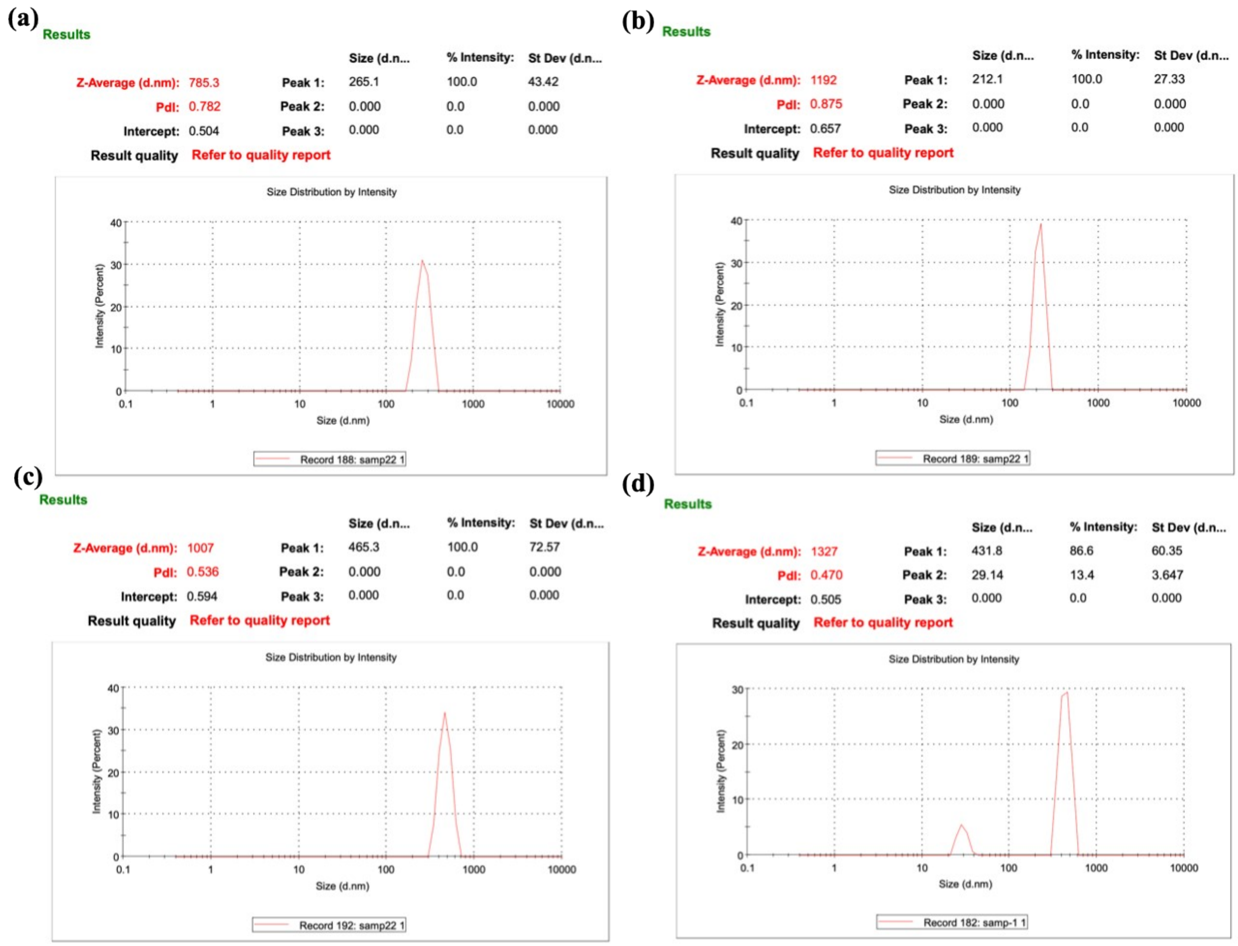

Figure S5: Dynamic light scattering (DLS) analysis of silk silver fibroin solution prepared with different $AgNO_3$ concentrations. (a) 0.25%, (b) 0.5% samples exhibit narrow, unimodal intensity distributions with peak hydrodynamic diameters of 265.1 nm and 212.1 nm, respectively, indicating homogeneous and stable nanocluster assemblies. In contrast, (c) the 0.75% and (d) 1% formulations show broadened or multimodal size distributions, with peak sizes shifting to 465.3 nm and 431.8 nm, respectively, reflecting increased polydispersity and early aggregation. These results confirm that $AgNO_3$ concentrations above 0.5% exceed the stabilizing capacity of silk fibroin, leading to loss of uniform nanocluster formation.

Sample Name	Day 1 (Weight in mg)	Day 7 (Weight in mg)
Silk Film	78.2 ± 0.5 mg	77.9 ± 0.4 mg
Silk-Silver Film	89.4 ± 0.6 mg	110.2 ± 0.8 mg

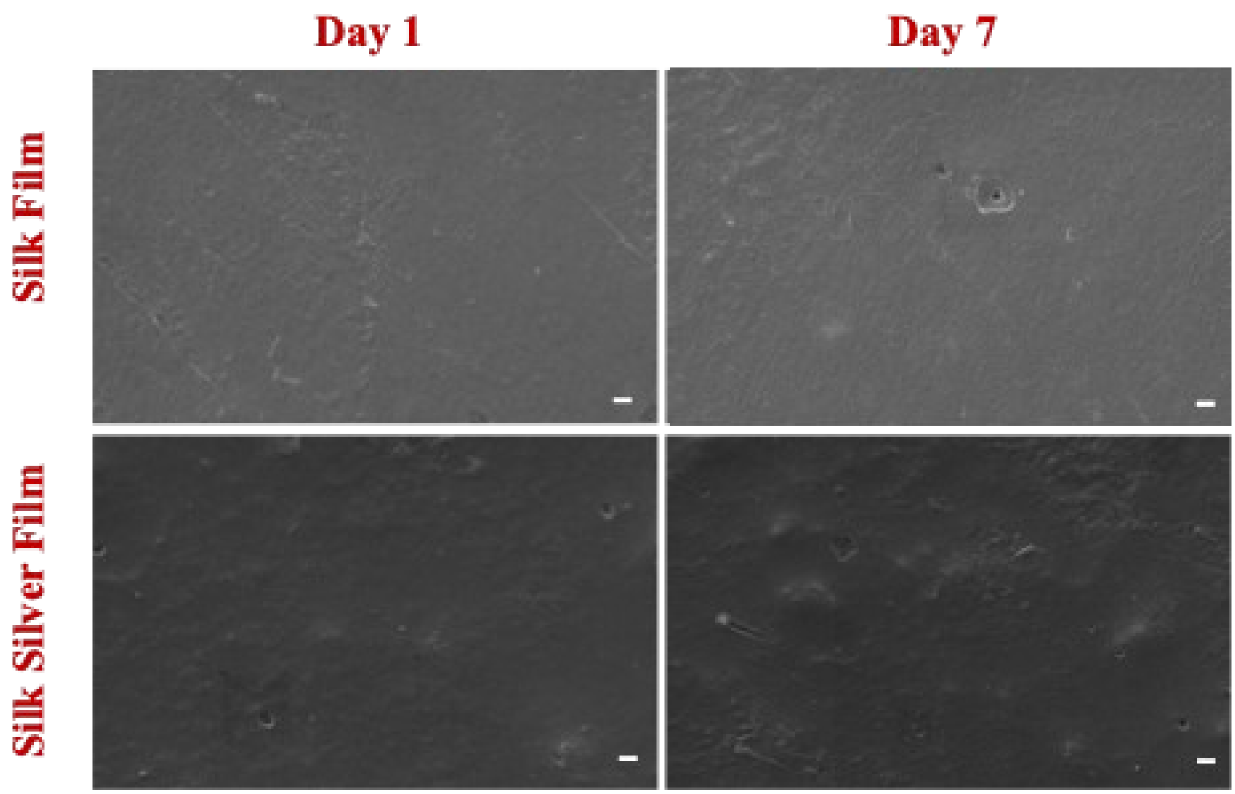

Figure S6: SEM images of the silk film, silk silver films at day 1 and day 7 to observe the biodegradability of the films when incubated in cell culture media (DMEM) for 7 days at 37 ^{0}C. (Scale:2 µm)

References:

1. Zhang, Y. *et al.* Biomimetic Inorganic Nanoparticle-Loaded Silk Fibroin-Based Coating with Enhanced Antibacterial and Osteogenic Abilities. *ACS Omega* 6, 30027–30039 (2021).
2. Pollini, M., D'Urso, F., Broccolo, F. & Paladini, F. Silver Nanoparticle–Silk Protein Nanocomposites: A Synergistic Biomimetic Approach for Advanced Antimicrobial Applications. *Biomimetics* 10, 669 (2025).
3. Felemban, M. *et al.* Extracellular matrix component expression in human pluripotent stem cell-derived retinal organoids recapitulates retinogenesis in vivo and reveals an important role for IMPG1 and CD44 in the development of photoreceptors and interphotoreceptor matrix. *Acta Biomater* 74, 207–221 (2018).
4. He, H. *et al.* In situ green synthesis and characterization of sericin-silver nanoparticle composite with effective antibacterial activity and good biocompatibility. *Materials Science and Engineering: C* 80, 509–516 (2017).
5. Al Masud, Md. A. *et al.* Green synthesis of silk sericin-embedded silver nanoparticles and their antibacterial application against multidrug-resistant pathogens. *Journal of Genetic Engineering and Biotechnology* 19, 74 (2021).